ACS APPLIED ENERGY MATERIALS

www.acsaem.org Article

PEDOT-Based Stackable Paper Electrodes for Metal-Free Supercapacitors

Luciano D. Sappia,[‖] Blanca Sol Pascual,[‖] Omar Azzaroni, and Waldemar Marmisollé*

Cite This: *ACS Appl. Energy Mater.* 2021, 4, 9283−9293 Read Online

ACCESS | Metrics & More | Article Recommendations | Supporting Information

ABSTRACT: Paper-based electrodes are promising candidates for energy storage devices due to its availability in nature, low cost, sustainability, intrinsic porosity/fibrous structure, and mechanical properties. In this work, we implemented a straightforward method to control the capacitive response of paper electrodes modified by deposition of PEDOT-polyamine composites. These composite materials were characterized by TGA, SEM-EDS, and Raman spectroscopy, proving the homogeneous functionalization and proper integration of the polymers within the paper microstructure. The electrochemical evaluation by cyclic voltammetry (CV) and galvanostatic charge−discharge curves (GCD) revealed the stable electroactivity of the paper electrodes in a neutral 0.5 M NaCl solution, whereas the introduction of polyamine yielded an enhancement of the capacitive performance. Furthermore, the stacking of paper sheets on a current collector was proved to be an efficient strategy for building electrodes with tunable pseudocapacitance with adequate electrochemical connectivity across the whole architecture. A linear increase in the total capacitance measured by both CV and GCD (60−400 mF/cm^2) on the number of stacked PEDOT-modified paper sheets was determined (1−6 sheets). The stacking strategy was comparatively tested using both plastic (PET) and metallic (Au) substrates for preparing the current collectors with similar results and excellent cyclability and capacitance retention (97% after 1000 GCD cycles for three stacked sheets) in 0.5 M NaCl as a harmless and environmentally friendly electrolyte. The stacking of paper sheets modified by polyamine-doped PEDOT coatings constitutes a simple and promissory strategy facing the construction of lightweight metal-free electrodes for harmless supercapacitors in wearable devices.

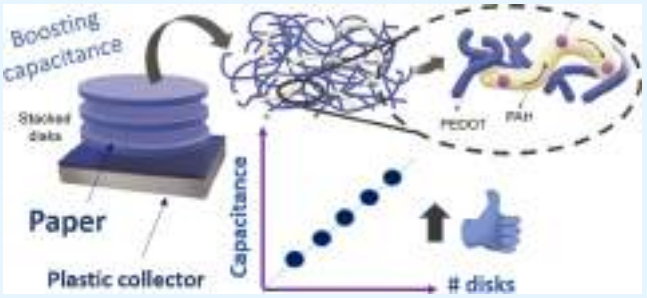

KEYWORDS: *PEDOT, supercapacitors, energy storage, electrochemistry, paper electrodes, stackable electrodes, conducting polymers, metal-free devices*

1. INTRODUCTION

In the last few decades, the limitation of nonrenewable energy sources has increased the need for new alternative energy storage solutions.[1] This has also led to the growing development of efficient energy storage devices, including new batteries, capacitors, and supercapacitors.[2] Due to their remarkable properties, supercapacitors (SCs) can be classified between classical batteries and capacitors.[3−5] SCs store higher energy densities than capacitors and manage higher power densities than batteries, making them an optimal option for devices that require short charge/discharge times and moderate charge storage.[6]

According to the charge storage mechanism, SCs are classified in electrical double-layer capacitors (EDLCs), pseudo- or redox capacitors, and hybrid SCs. In EDLCs, the charge is stored by electrostatic interactions of the ions on each electrode and no chemical reactions take place (non-faradic process). The physical adsorption of charged molecules occurs rapidly, providing high charge/discharge rates and good cyclability but low energy densities due to the surface availability limitations.[2,7] Highly porous carbon materials are commonly used in these devices, in which the accessible surface and the pore size are key parameters.[8] On the other hand, pseudocapacitors store the charge by means of rapid and reversible redox reactions on the electrode material (faradic process), leading to higher charge densities but lower cyclability than EDLCs. Finally, hybrid SCs combine EDLC and pseudocapacitance mechanisms.[6] Thus, the integration of conducting materials is required for any storage application. Carbon materials, metal oxides, and conducting polymers have been extensively employed for the fabrication of SCs.[4,9−12] For instance, some examples include the use of MnO_2 thin films for the fabrication of flexible SCs using gel electrolytes,[13] MnO_2 nanowires on activated carbon for all-solid-state SCs,[14] and VO_2 nanosheets electrodes in organic gel electrolytes.[15] Within

Received: May 28, 2021
Published: September 2, 2021

https://doi.org/10.1021/acsaem.1c01517
ACS Appl. Energy Mater. 2021, 4, 9283−9293

conducting polymers, polypyrrole (Ppy),[16] polyaniline (PANI),[17−19] poly(3,4-ethylenedioxythiophene) (PEDOT), and their derivatives have been extensively used in redox capacitors.[20−24] Particularly, PEDOT-based SCs have received great attention in the last few years due to their outstanding electrical properties, in addition to their high specific capacitance, flexibility biocompatibility, acceptable potential window for electrochemical operation, air stability, superior chemical stability in the doped state, and a small band gap.[25−29] Most of the aforementioned materials require the use of conductive substrates as ITO or carbon materials as current collectors.[30] Even the use of carbon cloth has also been reported for both a mechanical scaffold and a current collector.[21,31] However, in the case of PEDOT, it is possible to produce metal-free electrodes by depositing conducting polymer films on insulating plastic substrates, with excellent performance in electrochemical applications such as nanofluidics,[32] biosensing,[33,34] and even for flexible electrodes.[35,36]

Although conducting polymers provide huge redox-type pseudocapacitances, mechanical tensions due to intrinsic volume changes upon redox switching can lead to material breakdown in operation.[37] Thus, the incorporation of structural scaffolds is sometimes needed for achieving appropriate mechanical stability. In this regard, cellulose fibers or paper sheets become interesting options as structural scaffolds for the construction of hybrid materials in energy storage applications.[38−40] Paper substrates are easily available, sustainable, and environmentally friendly. In addition, they can be recycled from multiple sources, leading to low fabrication costs and they are compatible with mass production techniques.[41] The intrinsic large porous surface of paper electrodes allows high mass loading of conductive materials and composites, which renders better capacitive performance in energy storage devices.[42] On the other hand, the use of insulating materials as scaffolds could also produce the disruption of electronic pathways along the electrode material, causing partial electrochemical blockage and lowering the amount of the electroactive material that is effectively connected to the current collector. Therefore, a proper integration of the electroactive material across the paper substrate becomes a requisite for developing efficient supercapacitors.

Concerning the nature of the electrolyte used in supercapacitors, organic electrolytes allow using higher operating voltages yielding higher energy densities, but they also have some disadvantages related to their toxic nature and polluting production. Alternatively, aqueous electrolytes typically include highly acidic or basic solutions as required by the nature of the electroactive components of the electrode material. Some disadvantages of employing highly acidic or basic electrolytes are related to environmentally unfriendly production, corrosive nature, and the risks of injuries when employed in wearable applications. In this regard, neutral solutions of common inorganic salts have been proposed as more environmentally friendly and harmless alternatives,[43] particularly in the case of the low-cost and widely available KCl and NaCl solutions.[13,44]

The occurrence of redox commutation in conducting polymers requires the movement of electrons along the polymer chains and also the ionic transport to compensate charges within the electroactive coating.[45,46] This implies that the electrolyte needs to penetrate the interior of the electroactive material microstructure to allow an efficient ion movement coupled to the electronic transport. In the case of aqueous solutions, movements of both ions and water molecules take place through hydrophilic domains or channels. Then, the modulation of the hydrophilic domains within the electroactive composite is also important for maximizing the capacitive response of conducting polymer-based supercapacitor materials. This phenomenon has been extensively studied for PEDOT-based materials in organic field-effect transistors,[47−50] where the integration of polyelectrolytes to the PEDOT matrix has been shown to produce an improvement of the ion mobility. Particularly, the integration of polyallylamine hydrochloride (PAH) within PEDOT:tosylate films has been recently reported to improve the transient response of the organic transistors due to an enhancement of the ionic transport compared with unmodified PEDOT:tosylate films.[51]

In this context, we introduce a strategy based on the stacking of paper electrodes embedded with composites of PEDOT and PAH for the construction of electrode materials for SCs working in a neutral NaCl solution. The electroactive paper is prepared by in situ chemical polymerization of EDOT by ferric tosylate in the presence of PAH on cellulose fibers. By this functionalization procedure, the composite is homogenously integrated within the paper microstructure, yielding paper electrodes with outstanding electroactivity and stability in aqueous solution. The addition of PAH to the polymerization formulation increases the areal capacitance of the resulting paper electrodes. The good electrical conductivity of the modified paper allows for the construction of thicker electrodes by direct stacking of the paper sheets on a current collector, yielding electrodes with a linear increase in the areal capacitance on the number of stacked sheets. The stacked configuration was also tested with a PEDOT-coated plastic substrate as a current collector, producing metal-free electrodes with high cyclability and capacitance retention in 0.5 M NaCl solutions.

2. EXPERIMENTAL DETAILS

2.1. PEDOT Synthesis. PEDOT-coated paper substrates were prepared by in situ polymerization of 3,4 ethylendioxythiophene (EDOT) monomer solutions spin-coated on paper substrates, following a protocol previously reported by our group and others.[33,52−54] The polymeric composites were directly spin-coated on paper sheets (5 cm × 5 cm, thickness = 180 μm, pore size = 11 μm, Whatman grade 1, GE Healthcare). Neither chemical nor physical treatments were applied to the commercial paper sheets before the deposition of the polymerization solution. In parallel, the deposition was carried out on glass and gold substrates for comparison. Previous to spin coating, an oxidant solution was prepared mixing 1830 μL of 40% iron(III) tosylate ($Fe(Tos)_3$) in butanol (CB 40, Clevios, Heraeus Holding GmbH, Hanau, Germany), 440 μL of butanol (ACS, Merck), and 33 μL of pyridine (ACS, Biopack). Then, 1900 μL of the oxidant solution was mixed with 25 μL of the EDOT monomer (97%, Sigma-Aldrich). This solution was homogenized in a vortex and filtered (pore diameter: 0.2 μm). The deposition was immediately carried out by spin coating (WS-650MZ-23NPP, Laurell) using the resultant mixture at 1000 rpm for 1 min and an acceleration of 500 rpm. Then, the substrates were heated at 70 °C for 15 min. In this step, the oxidative polymerization of EDOT took place, giving rise to a dark thin film of conductive PEDOT as a homogeneous coating for the paper substrate. These substrates were immersed twice in deionized water (DIW) for 5 min and thoroughly rinsed again with DIW to remove the excess oxidant. Finally, the substrates were dried in a hot plate at 70 °C for 15 min.

Composites of PEDOT and polyallylamine hydrochloride (PAH, MW = 58 kD, Sigma-Aldrich) were also synthesized onto paper

https://doi.org/10.1021/acsaem.1c01517
ACS Appl. Energy Mater. 2021, 4, 9283−9293

Scheme 1. (A) Preparation of PEDOT and PEDOT-PAH Composites on the Paper Sheets by Spin Coating; (B) Chemical Structure of PEDOT; and (C) Representation of the Introduction of PEDOT-PAH on the Cellulose Substrates

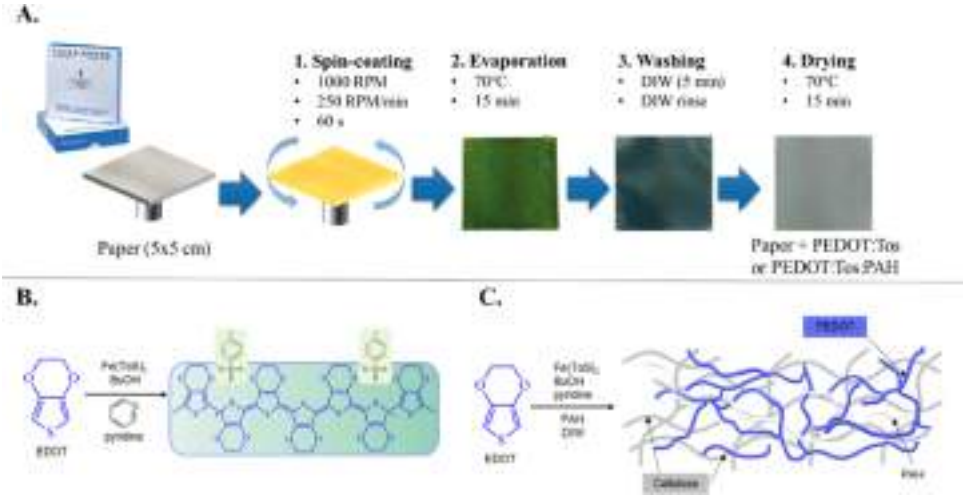

following the same protocol used for pristine PEDOT deposition with minimal modifications. First, PAH (30 mg) was dissolved in 400 μL of DIW. The solution was heated at 30 °C for some minutes and vortexed until PAH was completely dissolved. Second, 1830 μL of the oxidant solution was added to the PAH solution and mixed vigorously. Finally, the EDOT monomer was added into the polymerization solution and the resultant solution was filtered and deposited on the paper substrates by spin coating.

2.2. Characterization. *2.2.1. Raman Spectroscopy.* Raman spectra were acquired using an i-Raman BW415-532S (BWTek) Raman spectrometer using a laser (λ = 532 nm) focused on the substrates by a 20× optical microscope (BAC151B, BWTek). The operative power was 10 mW and the spectral region analyzed ranged from 100 to 4000 cm^{-1}. For comparison, the PEDOT and PEDOT-PAH samples were deposited on glass substrates to avoid the intrinsic peaks associated with the paper substrate.

2.2.2. SEM. SEM micrographics were taken using an FEI Quanta 600 scanning electron microscope. Each sample was coated with sputtered gold to assure the electrical conductivity of the surface. The section and surface were analyzed for each sample. EDS was also carried out.

2.2.3. TGA. Thermogravimetric analysis (TGA, TA Instruments) was employed to access the relative composition of polymer PEDOT and PEDOT-PAH within the paper substrates. The samples were identically subjected to TGA at a heating rate of 10 °C/min under a N_2 environment. To calculate the mass ratio between the polymer and the paper substrate, the samples were cut in disks (n = 3, diameter = 3 mm), heated at 100 °C for 10 min in N_2, and comparatively weighed in the TGA analytical balance. Then, the polymer mass deposited was calculated as the difference between the composite-coated paper and the pristine paper sample.

2.3. Electrochemistry. Cyclic voltammetry (CV) and galvanostatic charge−discharge experiments (GCD) were performed with a Reference 600 potentiostat (Gamry Instruments) using a three-electrode cell configuration equipped with a Ag/AgCl (3 M NaCl) reference electrode, a platinum mesh counter electrode, and a working electrode with an exposed area of 0.178 cm^2. PEDOT and PEDOT-PAH composites were individually evaluated by CV in 0.5 M NaCl. Scans were performed from 0 to 0.8 V at different scan rates from 5 to 100 mV/s. The GCD measurements were performed at different current densities (0.5−8 mA/cm^2). The stability of the arrangement of the stacked electrodes was evaluated using PEDOT or PEDOT-PAH layers deposited on both gold and PET current collectors performing up to 1000 GCD cycles at 4 mA/cm^2.

The voltammetric areal capacitance (C_{CV}) was computed as

$$C_{CV} = \frac{Q_{CV}}{\Delta V_{CV} \cdot A} \quad (1)$$

where Q_{cv} means the voltammetric integrated charge for the anodic scan, ΔV_{cv} is the potential window of the voltammetric scan, and A is the geometrical value of the electrode area exposed to the electrolyte solution.

On the other hand, the areal capacitance obtained from GCD experiments (C_{GCD}) was computed as[23]

$$C_{GCD} = \frac{I \cdot t}{\Delta V \cdot A} \quad (2)$$

where I means the constant current value employed, t is discharging time, and ΔV is the potential window. Areal energy density and areal power density values were computed as[55]

$$E_D = \frac{C_{GCDI} \cdot V^2}{2 \cdot 3600} \quad (3)$$

$$P_D = \frac{3600 \cdot E_D}{\Delta t} \quad (4)$$

where V is the working voltage.

3. RESULTS AND DISCUSSION

PEDOT and PEDOT-PAH composites were deposited on paper substrates by spin coating. The parameters for the deposition were optimized from our previous experiments using plastic substrates such as acrylic and poly(ethylene terephthalate) (PET) sheets.[34] Shortly, 5 × 5 cm^2 paper samples are attached on an acrylic base and the deposition solution is poured on top until it is distributed on the entire surface by capillarity. Then, the sample is spin-coated, heated, washed, and dried, as shown in Scheme 1. For the case of the PEDOT-PAH composite, the same procedure was followed by dissolving PAH in DIW before mixing with the oxidant and monomer solutions. The polymer deposition procedure can be repeated several times to create multilayer coatings with high reproducibility. In this way, different composites and combinations were evaluated, as summarized in Table 1.

3.1. Physicochemical Characterization. *3.1.1. Sheet Resistance.* Conductivity characterization by a four-point probe was performed for different composite materials (see the SI for details). The results corresponding to five different positions on each sample are reported in Figure 1A. From the

https://doi.org/10.1021/acsaem.1c01517
ACS Appl. Energy Mater. 2021, 4, 9283−9293

Table 1. PEDOT and PEDOT-PAH Composites Deposited on Paper Substrates

name	composition
P_{1L}	one layer of pristine PEDOT
P_{2L}	two layers of pristine PEDOT
P_{3L}	three layers of pristine PEDOT
P-PAH_{1L}	one layer of PEDOT-PAH composite
P-PAH_{2L}	two layers of PEDOT-PAH composite
P-PAH_{3L}	three layers of PEDOT-PAH composite
P_{2L} P-PAH_{1L}	two layers of pristine PEDOT and one layer of PEDOT-PAH composite

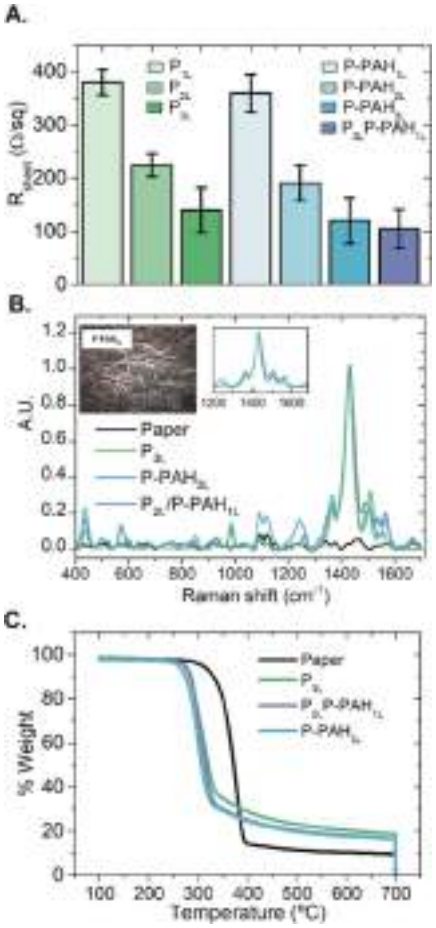

Figure 1. (A) Sheet resistance of P_{1L}, P_{2L}, P_{3L}, P-PAH_{1L}, P-PAH_{2L}, P-PAH_{3L}, and P_{2L}P-PAH_{1L} measured by a four-probe sensor. (B) Raman spectra (λ = 532 nm) of neat paper, P_{3L}, P-PAH_{3L}, and P_{2L} P-PAH_{1L} samples. Inset: optical microscopy image (20×). (C) TGA experiments in N_2 of pristine paper, P_{3L}, P-PAH_{3L}, and P_{2L} P-PAH_{1L} samples.

results shown in Figure 1A, it is clear that an increase in the number of coating steps leads to a decrease in the sheet resistance (R_{sheet}) of the sample for both pristine PEDOT and PEDOT-PAH composites. The homogeneity and low R_{sheet} values obtained in the sample coated with two layers of pure PEDOT and a third one of the PEDOT-PAH composite (P_{2L} P-PAH_{1L}) are also very noticeable.

We have also explored the drop-casting deposition method as a simpler alternative to spin coating (see Section S1.2). Using 50−100 μL of the deposition solution, the R_{sheet} values were in the order (100−400 Ω) of those of the P_{1L} films deposited by spin coating. However, higher homogeneity of the conductivity values was attained by the spin-coating method. For higher deposited volume, the sheet resistance values obtained by drop casting were even higher (Figure S1.2). Then, for homogeneity reasons, the spin-coating method was chosen as the paper functionalization procedure in this work.

3.1.2. Raman Spectroscopy. Figure 1B shows the Raman spectra of P_{3L}, P-PAH_{3L}, P_{2L} P-PAH_{1L}, and neat paper. The P_{3L} spectrum includes bands at 435.4 cm^{-1} due to SO_2 bending; 570.8 cm^{-1} is assigned to oxyethylene ring deformation; 691.2 cm^{-1} due to the symmetric C−S−C deformation; 986.7 cm^{-1} due to the oxyethylene ring deformation; 1090.3 cm^{-1} related to C−O−C deformation; 1262.83 cm^{-1} assigned to the C_α−C_α inter-ring stretching; 1364.6 cm^{-1} related to C_β−C_β stretching; 1427.4 cm^{-1} due to the symmetric C_α = C_β(−O) stretching; and 1558.4 cm^{-1} assigned to the asymmetric C_α−C_β stretching. These main bands are also present in the spectra of the paper substrates functionalized by the PEDOT-PAH composite. Moreover, in the case of P-PAH_{3L} and P_{2L}/P-PAH_{1L}, the presence of PAH is related to the distortion of the band at about 1500 cm^{-1} (caused by the superposition of the symmetric and antisymmetric bending bands of protonated amines), and the broadening of the band at 1360 cm^{-1} is assigned to CH bending modes (inset of Figure 1B). All these signals agree with the results obtained in previous works, confirming the presence of PEDOT and PAH.[33,34]

3.1.3. TGA and SEM Analysis. Figure 1C shows the results from experiments carried out in a N_2 atmosphere. The samples of functionalized papers are thermally stable at least up to 250 °C, and the stability slightly decreases with the proportion of PAH. On the other hand, the integration of PEDOT and the PEDOT-PAH composite occurs in the lower volatility of the thermal decomposition products, as a higher proportion of the material remains on the plate at high temperatures. From mass values determined for pristine and modified paper substrates, the amount of the active material was determined to be ca. 1 mg/cm^2 for all these coatings. This result indicates that approximately the same mass of the material is deposited after one deposition step, independent of the nature of the spin-coating solution.

This is also consistent with the similar appearance observed in the SEM images for PEDOT and PEDOT-PAH-functionalized paper substrates (Figure 2). As observed in SEM images, the structure of the paper fibrils remains after coating with PEDOT and PEDOT-PAH and there are no appreciable differences between PEDOT and PEDOT-PAH at this microscopic level (see the SI for additional SEM and EDS analysis). EDS analysis performed at different locations on the samples also reveals a highly homogeneous coating composition (Section S1.3).

From the physicochemical characterization, it can be stated that the present spin-coating procedure becomes an effective method for the integration of PEDOT and PEDOT-PAH composites on paper substrates, yielding homogeneous coatings and preserving the initial fibril structure. The inclusion of the insulating polyelectrolyte does not drastically modify the electronic conductivity of the PEDOT-modified paper substrates and no structural differences are observed in the SEM analysis. However, differences at the molecular level can be inferred from the analysis of the electrochemical behavior of the functionalized paper substrates, as discussed in the next section.

https://doi.org/10.1021/acsaem.1c01517
ACS Appl. Energy Mater. 2021, 4, 9283−9293

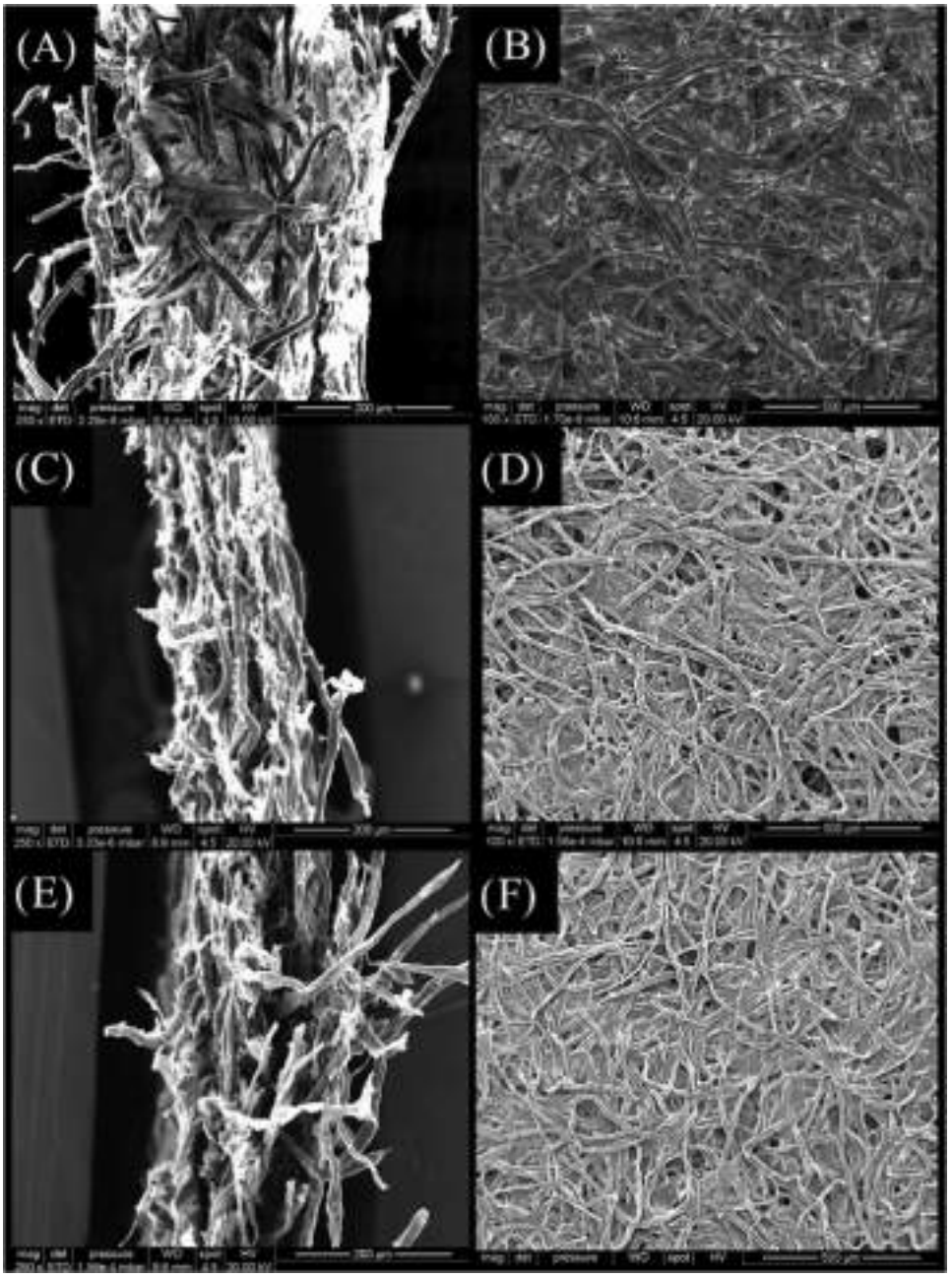

Figure 2. SEM micrographs corresponding to (A) cross section and (B) surface of pristine paper; (C) cross section and (D) surface of P_{3L}; and (E) cross section and (F) surface of P_{2L}P-PAH_{1L}.

3.2. Electrochemical Behavior of PEDOT and PEDOT-PAH-Modified Paper Electrodes. Paper electrodes were prepared as shown in Figure 3A. Briefly, the electrodes were constructed by cutting the paper substrate modified with PEDOT and PEDOT-PAH in 2 × 0.5 cm^2 strips. The active area of the electrode was fixed using a wax layer as a hydrophobic barrier. Silver paint was used to ensure an electrical connection with potentiostat connectors. To enhance the mechanical stability, paper samples were attached to glass slides using double-sided tape. However, note that no current collector is used in this configuration, and the electrical connection between the active area and the silver paint contact (about 1.5 cm) is performed by the PEDOT-modified paper sheet. The electrolyte concentration was chosen based on its effect on the capacitive behavior of the P_{2L} sample while increasing the concentration from 0.1 to 0.5 M (Figure S2.1A). As the capacitive response increased with the NaCl concentration, a 0.5 M NaCl solution was selected for further experiments.

For voltammetric experiments, samples modified by three successive depositions of PEDOT or PEDOT-PAH were studied, as they presented the lowest sheet resistance. The electroactive area of each electrode was delimited using a wax barrier and then was cut, as shown in Figure 3A. Cyclic voltammograms (CV) corresponding to P_{3L}, P-PAH_{3L}, and P_{2L} P-PAH_{1L} paper electrodes in 0.5 M NaCl are presented in Figure 3B. Despite being metal-free paper electrodes, the voltammetric response is clearly defined, showing a capacitive behavior. The areal capacitance (C_{CV}) calculated from CVs at

https://doi.org/10.1021/acsaem.1c01517
ACS Appl. Energy Mater. 2021, 4, 9283−9293

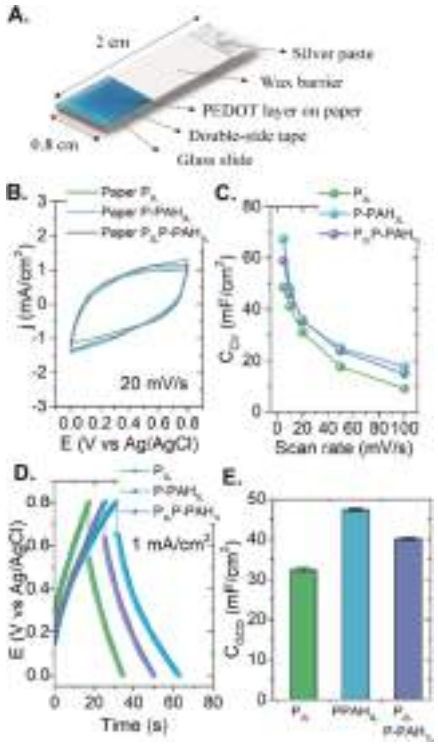

Figure 3. (A) Scheme of the PEDOT-modified paper electrode configuration. Capacitive performance of the P_{3L}, P-PAH_{3L}, and P_{2L}P-PAH_{1L} electrodes in 0.5 M NaCl. (B) Voltammograms at 20 mV/s. (C) C_{CV} at different scan rates. (D) GCD cycles at 1 mA/cm^2. (E) C_{GCD} calculated as the average from 10 discharge cycles.

different scan rates for these electrodes are reported in Figure 3C.

By comparing the results for the P_{3L}, P-PAH_{3L}, and P_{2L} P-PAH_{1L} paper electrodes, it can be stated that the presence of PAH in the composite leads to higher capacitance values, although it is not an electroactive component. The results of the physicochemical characterization of these materials presented in the previous section indicate that reasons are not related to the differences in the electronic conductivity (or sheet resistance) or the microscopic fibril structure. Then, the effect of the incorporation of the (insulating) polyelectrolyte into the conducting matrix on the electrochemical performance could be related to the enhancement of the ionic current. In this regard, it has been reported that the incorporation of polyelectrolytes into the PEDOT-based conducting matrix involves the formation of hydrophilic domains that facilitates ion percolation mechanisms, improving the performance in organic electrochemical transistor configuration. Such improvement of the ion mobility has been reported in the case of films of PEDOT:PSS, PEDOT:tosylate−gelatin, and other composites as conducting channels in organic electrochemical transistors.[47−49] Also an enhancement of the percolation pathway by addition of cationic polyelectrolytes into PEDOT:PSS films has been reported.[50] Particularly, the integration of hydrophilic domains formed by positively charged polyelectrolytes to the PEDOT:tosylate composites is supposed to have a more pronounced effect than in the case of PEDOT:PSS films, as anion exchange from/to the solution becomes more important for charge compensation during the redox switching. In this regard, the integration of PAH has been recently shown to effectively increase the hydrophilicity and ionic conductivity within PEDOT:tosylate films in organic electrochemical transistor configuration.[51] Thus, in the present configuration, the introduction of hydrophilic domains could facilitate the anion transport inside the functionalized paper, yielding higher capacitance values.

On the other hand, GDC curves were performed for the P_{3L}, P-PAH_{3L}, and P_{2L}P-PAH_{1L} paper electrodes in 0.5 M NaCl (Figure 3D). Mean capacitance values obtained from 10 GCD curves (C_{GCD}) are reported in Figure 3E. Once again, the best capacitive response is obtained in the case of the P-PAH_{3L} composite paper electrode.

Based on the best electrochemical response of the P-PAH_{3L} paper electrode, this functionalization scheme was employed for further studying the cyclability and the performance in the stacked configuration of the paper electrodes in the next sections.

3.3. Controlling Capacity by Stacking PEDOT-PAH-Modified Paper Sheets. After characterizing the capacitive behavior of the modified paper electrodes, we evaluated the stacking of paper sheets as a strategy for the construction of electrodes with controllable capacitance values. For these studies, P-PAH_{3L} paper sheets were employed, as they presented the best capacitive performance. Disks of modified paper sheets were cut and manually stacked without using any additional adhesive layer between them (Figure 4A). The diameter of these disks was higher than the diameter of the *o*-ring of the electrochemical cell, so the electroactive area evaluated was still constant and comparable among the different stacked configurations.

Despite the good electrochemical results in the CV experiments, the electrode configuration without the current collector presents a relatively high drop resistance in the GCD curves for the stacking studies. To overcome this issue, two alternative configurations were explored. On the one hand, metallic Au electrodes were modified by a PEDOT layer by spin coating (Figure S3.1). On the other hand, a metal-free plastic collector was built by depositing a PEDOT film on a PET slide. In this case, a thicker PEDOT film (three spin-coating routines) was deposited to allow reaching a voltammetric response comparable to that obtained with the Au collector (Figure S3.1).

The stacking strategy was first evaluated using the Au collector by cyclic voltammetry at increasing scan rates and by GCD at different current densities, as shown in Figure 4. As revealed by Figure 4B, the simple stacking of the PEDOT composite-modified paper sheets leads to an increase in the capacitive current. Moreover, at a low scan rate, the voltammetric capacitance linearly increases with the number of stacked paper disks (Figure 4C), proving the effectiveness of this strategy. The obtained C_{CV} ranged from ca. 50 to 300 mF/cm^2 at 10 mV/s by stacking 1−6 disks. The linear dependence indicates that in these experimental conditions, the total electrode areal capacitance can be easily tuned by stacking an adequate number of paper disks. Moreover, it suggests that the charge transfer across the whole stacked electrode is effective, and each paper sheet contributes equally to the total capacitance. Contrarily, at higher scan rate values, the linear trend drops off as the number of stacked disks is augmented (Figure S3.2), which suggests that the charge transport across the whole stacked electrode becomes slow compared with the potential scan rate.

Afterward, GCD cycles at 1 mA/cm^2 were applied for each stacked arrangement (Figure 4D) and the average values of

https://doi.org/10.1021/acsaem.1c01517
ACS Appl. Energy Mater. 2021, 4, 9283−9293

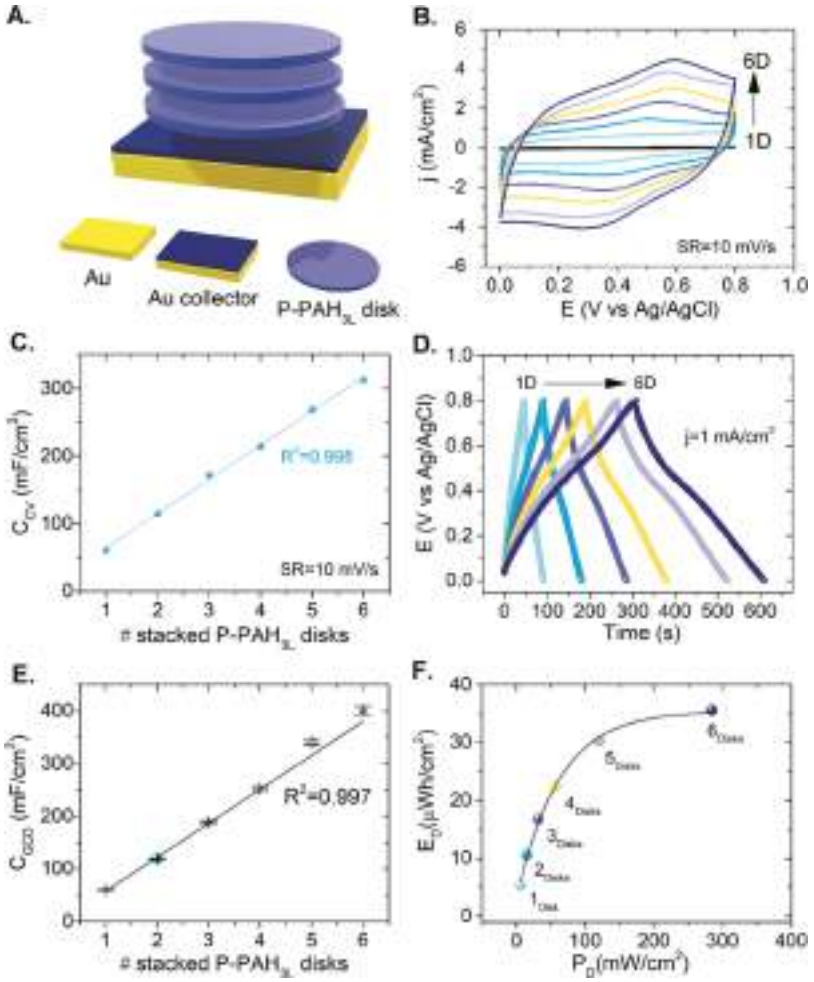

Figure 4. Capacitive behavior in the stacked configuration. Evolution of the capacitance in 0.5 M NaCl for an increasing number of stacked disks of P-PAH-modified paper sheets using the Au collector. (A) Scheme of the stacking strategy. (B) CV at 10 mV/s. (C) Voltammetric capacitances (C_{cv}) at 10 mV/s. (D) GCD cycles at 1 mA/cm^2. (E) Galvanostatic capacitances (C_{GCD}) obtained from (D). (F) Ragone's plot for the stacking of 1−6 P-PAH$_{3L}$-modified paper disks on the Au current collector.

C_{GCD} of 10 consecutive cycles are reported in Figure 4E. In this case, the C_{GCD} values linearly increased from 60 to 400 mF/cm^2 for 1−6 stacked disks at 1 mA/cm^2, in agreement with voltammetric data at low scan rates. These data from GCD curves were also represented in Ragone's plot (Figure 4F), corresponding to E_D values ranging from 5 to 35 μWh/cm^2.

After evaluating the stacking strategy on the Au current collector, we explored another approach using a plastic collector. The performance of the Au and PET substrates coated with PEDOT as current collectors was comparatively evaluated by CV (see Section S3.3). The voltammetric responses obtained in these experimental conditions with the plastic and Au collectors are practically the same for the configuration with three stacked P-PAH$_{3L}$-modified paper disks (Figure S3.3). The voltammetric capacitance values obtained for both collectors are also comparable, as presented in Figure 5A. The capacitive performances are also comparable in terms of GCD curves. Figure 5B presents the GCD curves at current densities ranging from 0.5 to 8 mA/cm^2 for the electrode configuration with three stacked P-PAH$_{3L}$-modified paper disks using Au and PET current collectors. These similar results indicate that the use of the plastic substrate in the construction of the current collector does not limit the capacitive response of the stacked configuration. The same trends are also observed in Ragone's plot for both collectors for different current densities, reaching energy densities of 10 μWh/cm^2 with power densities of 420 and 550 mW/cm^2 for Au and PET collectors, respectively (Figure 5C).

The robustness of the stacking strategy was evaluated using continuous GCD cycles at a fixed current density of 4 mA/cm^2. Using the former configuration with three stacked P-PAH$_{3L}$-modified paper disks, capacitance retentions of 91 and 97% after 1000 cycles were obtained for the Au and PET collectors, respectively (Figure 6).

According to these results, the PET substrate coated with PEDOT can be effectively employed as a current collector, reaching a performance comparable to that obtained with metallic collectors.

Finally, the comparison of the present results with similar reported systems is presented in Table 2. As commented above, cellulose paper has been extensively used as a substrate for the preparation of electrodes. In this regard, many supercapacitor materials have been developed using cellulosic derivatives in the form of plain paper or fibers. Some of these systems are summarized in Table 2 for illustrating the wide variety of materials and electrolyte conditions. As concluded from the data presented in this table, the present system based on the PEDOT-PAH paper disks stacking on the PET current

https://doi.org/10.1021/acsaem.1c01517
ACS Appl. Energy Mater. 2021, 4, 9283−9293

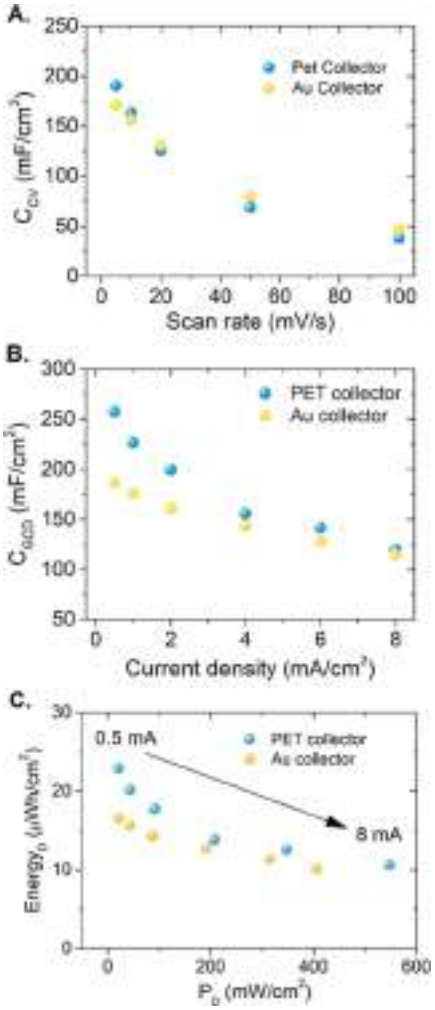

Figure 5. Comparison of the supercapacitor performance of the stacked electrode configuration using Au and PET current collectors. All data correspond to the stacking of three P-PAH$_{3L}$-modified paper disks. (A) Voltammetric capacitances at different scan rates. (B) Areal capacitances from GCD at increasing current densities (0.5, 1, 2, 4, 6, and 8 mA/cm^2). (C) Ragone's plot for the stacked electrodes using both collectors at increasing current densities (0.5−8 mA/cm^2).

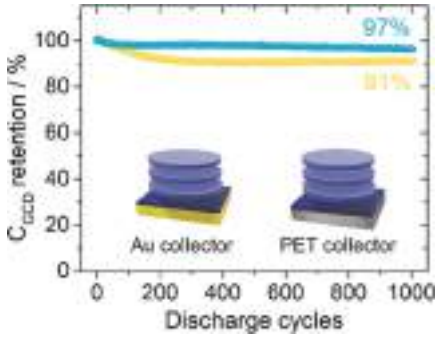

Figure 6. Long-term cycling stability for the electrode configuration using three stacked P-PAH$_{3L}$-modified paper disks on (yellow) Au and (blue) PET current collectors at 4 mA/cm^2.

collector showed an equivalent efficiency in terms of areal capacitance compared with other similar systems. However, it is important to highlight that the use of a harmless electrolytic solution such as aqueous NaCl can lead to the development of

Table 2. Comparison of the Performance of Supercapacitors Based on Paper or Cellulose Fibers

cellulose form	active material	electrolyte	C_{areal}	$C_{specific}$	Ragone data	references
paper	CNTs/MnO_2	poly(vinyl alcohol) (PVA)/KOH gel	123 mF/cm^2 (at 1 mA/cm^2)			40
fibers	PEDOT:PSS MWCNT	KOH and H_2SO_4		485 F/g at 1 A/g	E_D: 4.86 Wh/kg at P_D: 4.99 kW/kg	56
nanofibrils	PEDOT:PSS sulfonated lignin	$HClO_4$ 0.1 M in water/acetonitrile	1 F/cm^2	230 F/g		22
office paper	Zn and Ag powder-based screen printable pastes	KOH 5 M	0.166 mAh/cm^2 at 1 mA			57
filter paper	CNTs, zinc oxide and ferro ferric oxide	KOH 1 M		100.19 F/g at 5 A/g	E_D: 90.17 Wh/kg, P_D: 68.70 kW/kg	58
paper	PEDOT	PVA/H_2SO_4		179 F/g at 10 mV/s	E_D: 0.76 mWh/cm^3, P_D: 0.01 W/cm^3	23
paper	PEDOT	H_2SO_4 1 M	639 mF/cm^2			59
fibers	PEDOT and Alizarin red S	H_2SO_4 1 M	2191.3 mF/cm^2		E_D: 4.87 mWh/cm^3, P_D: 36 mW/cm^3	39
eggshell membranes	PEDOT/carbon nanostructures	PVA−H_3PO_4	36.9 mF/cm^2	58.4 F/g		60
paper	PEDOT and PAH	NaCl 0.5 M	400 mF/cm^2 (at 1 mA/cm^2)	67 F/g (6-disk stacking)	E_D: 35 μWh/cm^2, P_D: 300 mW/cm^2	this work

https://doi.org/10.1021/acsaem.1c01517
ACS Appl. Energy Mater. 2021, 4, 9283−9293

both safe and environmentally friendly energy storage devices in comparison with organic solvents or highly acidic solutions.

Additionally, in the stacked configuration with PET collectors, no metal contacts are needed. In this regard, the stability of the metal-free PET collector was better than using the gold collector after 1000 CDG cycles (97 and 91%, respectively). On the other hand, the use of PET as a current collector has several comparative advantages for the construction of electrodes for energy storage devices related to its low cost, low weight, and flexibility. Thus, the present method becomes a suitable alternative for the construction of wearable devices.

4. CONCLUSIONS

We have presented a simple strategy for developing electroactive materials for environmentally friendly neutral supercapacitors. First, we have shown that the integration of the cationic polyelectrolyte PAH results in an improvement of the areal capacitance of the paper electrodes. This improvement is ascribed to the enhancement of the ionic transport promoted by the inclusion of hydrophilic domains when integrating polyamine to the hydrophobic structure of PEDOT-based materials. Moreover, these paper electrodes are electroactive and electrochemically stable in a 0.5 M NaCl electrolyte.

Second, we have developed an affordable and practical strategy to control the areal capacitance by simple stacking of PEDOT/PAH-coated paper sheets. This simple method sets an innovative alternative for the manufacturing of supercapacitors with tunable areal capacitance. In this regard, areal capacitances of about 400 mF/cm^2 were obtained by stacking six P-PAH$_{3L}$-coated paper sheets on a gold substrate. Moreover, a plastic current collector was also evaluated; for this aim, three layers of PEDOT were spin-coated on a PET substrate. The electrical performance of the PEDOT-coated PET collector produced equivalent results to the Au collector. The stability of the stacked disk strategy showed a retention of 97% of its initial capacitance after 1000 GCD cycles at a current density of 4 mA/cm^2 using the PET collector.

Finally, the strategy presented in this work could be easily implemented for the construction of environmentally friendly energy storage devices at a large scale, by tuning both the number of coating steps for each paper sheet and the number of paper sheets in the stacked configuration. Also, the strategy developed based on the stacking of paper sheets functionalized with a PEDOT composite is also compatible with the use of plastic current collectors, which could be applied to the design and construction of energy storage devices for wearable applications.

■ ASSOCIATED CONTENT

Supporting Information

The Supporting Information is available free of charge at https://pubs.acs.org/doi/10.1021/acsaem.1c01517.

Experimental details and additional characterization of the PEDOT-PAH composites; voltammetric studies of the PEDOT and PEDOT-PAH paper disks in a three-electrode electrochemical cell; and evaluation of the stacked configuration (PDF)

■ AUTHOR INFORMATION

Corresponding Author

Waldemar Marmisollé − *Instituto de Investigaciones Fisicoquímicas Teóricas y Aplicadas, Departamento de Química, Facultad de Ciencias Exactas, Universidad Nacional de La Plata, CONICET, 1900 La Plata, Argentina;* orcid.org/0000-0003-0031-5371; Email: wmarmi@inifta.unlp.edu.ar

Authors

Luciano D. Sappia − *Instituto de Investigaciones Fisicoquímicas Teóricas y Aplicadas, Departamento de Química, Facultad de Ciencias Exactas, Universidad Nacional de La Plata, CONICET, 1900 La Plata, Argentina;* Present Address: Eurecat, Centre Tecnológic de Catalunya, 08290 Barcelona, Spain

Blanca Sol Pascual − *Instituto de Investigaciones Fisicoquímicas Teóricas y Aplicadas, Departamento de Química, Facultad de Ciencias Exactas, Universidad Nacional de La Plata, CONICET, 1900 La Plata, Argentina; Grupo de Polímeros, Área de química Orgánica, Facultad de Ciencias de la Universidad de Burgos, 09001 Burgos, España*

Omar Azzaroni − *Instituto de Investigaciones Fisicoquímicas Teóricas y Aplicadas, Departamento de Química, Facultad de Ciencias Exactas, Universidad Nacional de La Plata, CONICET, 1900 La Plata, Argentina;* orcid.org/0000-0002-5098-0612

Complete contact information is available at: https://pubs.acs.org/10.1021/acsaem.1c01517

Author Contributions

‖L.D.S. and B.S.P. contributed equally to this work. The manuscript was written through contributions of all authors. All authors have given approval to the final version of the manuscript.

Notes

The authors declare no competing financial interest.

■ ACKNOWLEDGMENTS

The authors acknowledge financial support from ANPCyT (PICT-2016-1680, PICT-2018-0780), Universidad Nacional de La Plata (PID-X867). W.M. and O.A. are CONICET staff members. B.S.P. acknowledges a scholarship from MINECO. L.D.S. gratefully acknowledges CONICET for the scholarship.

■ REFERENCES

(1) Salameh, M. G. Can Renewable and Unconventional Energy Sources Bridge the Global Energy Gap in the 21st Century? *Appl. Energy* **2003**, *75*, 33−42.

(2) Chen, H.; Cong, T. N.; Yang, W.; Tan, C.; Li, Y.; Ding, Y. Progress in Electrical Energy Storage System: A Critical Review. *Prog. Nat. Sci.* **2009**, *19*, 291−312.

(3) Chen, G. Z. Supercapacitor and Supercapattery as Emerging Electrochemical Energy Stores. *Int. Mater. Rev.* **2017**, *62*, 173−202.

(4) González, A.; Goikolea, E.; Barrena, J. A.; Mysyk, R. Review on Supercapacitors: Technologies and Materials. *Renewable Sustainable Energy Rev.* **2016**, *58*, 1189−1206.

(5) Conway, B. E. *Electrochemical Supercapacitors: Scientific Fundamentals and Technological Applications*; Springer, 1999.

(6) Simon, P.; Gogotsi, Y. Materials for Electrochemical Capacitors. *Nat. Mater.* **2008**, *7*, 845−854.

(7) Lei, C.; Wilson, P.; Lekakou, C. Effect of Poly(3,4-Ethylenedioxythiophene) (PEDOT) in Carbon-Based Composite Electro-

des for Electrochemical Supercapacitors. *J. Power Sources* **2011**, *196*, 7823−7827.
(8) Long, C.; Chen, X.; Jiang, L.; Zhi, L.; Fan, Z. Porous Layer-Stacking Carbon Derived from in-Built Template in Biomass for High Volumetric Performance Supercapacitors. *Nano Energy* **2015**, *12*, 141−151.
(9) Li, W.; Yuan, R.; Chai, Y.; Zhou, L.; Chen, S.; Li, N. Immobilization of Horseradish Peroxidase on Chitosan/Silica Sol−Gel Hybrid Membranes for the Preparation of Hydrogen Peroxide Biosensor. *J. Biochem. Biophys. Methods* **2008**, *70*, 830−837.
(10) Li, Q.; Horn, M.; Wang, Y.; MacLeod, J.; Motta, N.; Liu, J. A Review of Supercapacitors Based on Graphene and Redox-Active Organic Materials. *Materials* **2019**, *12*, No. 703.
(11) Kumar, M.; Sinha, P.; Pal, T.; Kar, K. K. *Materials for Supercapacitors*; Springer Series in Materials Science; Springer, 2020; Vol. *302*, pp 29−70.
(12) Zhou, H.; Ren, M.; Zhai, H.-J. Enhanced Supercapacitive Behaviors of Poly(3,4-Ethylenedioxythiophene)/ Graphene Oxide Hybrids Prepared under Optimized Electropolymerization Conditions. *Electrochim. Acta* **2021**, *372*, No. 137861.
(13) Moon, W. G.; Kim, G. P.; Lee, M.; Song, H. D.; Yi, J. A Biodegradable Gel Electrolyte for Use in High-Performance Flexible Supercapacitors. *ACS Appl. Mater. Interfaces* **2015**, *7*, 3503−3511.
(14) Mohammed, A. A.; Chen, C.; Zhu, Z. Green and High Performance All-Solid-State Supercapacitors Based on MnO2/ Faidherbia Albida Fruit Shell Derived Carbon Sphere Electrodes. *J. Power Sources* **2019**, *417*, 1−13.
(15) Rakhi, R. B.; Nagaraju, D. H.; Beaujuge, P.; Alshareef, H. N. Supercapacitors Based on Two Dimensional VO2 Nanosheet Electrodes in Organic Gel Electrolyte. *Electrochim. Acta* **2016**, *220*, 601−608.
(16) Zhao, J.; Wu, J.; Li, B.; Du, W.; Huang, Q.; Zheng, M.; Xue, H.; Pang, H. Facile Synthesis of Polypyrrole Nanowires for High-Performance Supercapacitor Electrode Materials. *Prog. Nat. Sci.: Mater. Int.* **2016**, *26*, 237−242.
(17) Wang, Y.; Mayorga-Martinez, C. C.; Pumera, M. Polyaniline/ MoS_x Supercapacitor by Electrodeposition. *Bull. Chem. Soc. Jpn.* **2017**, *90*, 847−853.
(18) Fenoy, G. E.; Van der Schueren, B.; Scotto, J.; Boulmedais, F.; Ceolín, M. R.; Bégin-Colin, S.; Bégin, D.; Marmisollé, W. A.; Azzaroni, O. Layer-by-Layer Assembly of Iron Oxide-Decorated Few-Layer Graphene/PANI:PSS Composite Films for High Performance Supercapacitors Operating in Neutral Aqueous Electrolytes. *Electrochim. Acta* **2018**, *283*, 1178−1187.
(19) Scotto, J.; Marmisollé, W. A.; Posadas, D. About the Capacitive Currents in Conducting Polymers: The Case of Polyaniline. *J. Solid State Electrochem.* **2019**, *23*, 1947−1965.
(20) Anothumakkool, B.; Soni, R.; Bhange, S. N.; Kurungot, S. Novel Scalable Synthesis of Highly Conducting and Robust PEDOT Paper for a High Performance Flexible Solid Supercapacitor. *Energy Environ. Sci.* **2015**, *8*, 1339−1347.
(21) Rajesh, M.; Raj, C. J.; Manikandan, R.; Chul, B.; Yeup, S.; Hyun, K. A High Performance PEDOT / PEDOT Symmetric Supercapacitor by Facile in-Situ Hydrothermal Polymerization of PEDOT Nanostructures on Fl Exible Carbon Fi Bre Cloth Electrodes. *Mater. Today Energy* **2017**, *6*, 96−104.
(22) Edberg, J.; Inganäs, O.; Engquist, I.; Berggren, M. Boosting the Capacity of All-Organic Paper Supercapacitors Using Wood Derivatives. *J. Mater. Chem. A* **2018**, *6*, 145−152.
(23) Li, B.; Lopez-Beltran, H.; Siu, C.; Skorenko, K. H.; Zhou, H.; Bernier, W. E.; Whittingham, M. S.; Jones, W. E. Vaper Phase Polymerized PEDOT/Cellulose Paper Composite for Flexible Solid-State Supercapacitor. *ACS Appl. Energy Mater.* **2020**, *3*, 1559−1568.
(24) Scotto, J.; Fenoy, G. E.; Sappia, L. D.; Marmisolle, W. A. Conducting Polymers-Based Electrochemical Platforms: From Biosensing to Energy Storage. *An. Asoc. Quim. Argent.* **2018**, *105*, 135−156.
(25) Kaur, G.; Adhikari, R.; Cass, P.; Bown, M.; Gunatillake, P. Electrically Conductive Polymers and Composites for Biomedical Applications. *RSC Adv.* **2015**, *5*, 37553−37567.
(26) Larsen, S. T.; Vreeland, R. F.; Heien, M. L.; Taboryski, R. Characterization of Poly(3,4-Ethylenedioxythiophene):Tosylate Conductive Polymer Microelectrodes for Transmitter Detection. *Analyst* **2012**, *137*, 1831.
(27) Lattach, Y.; Garnier, F.; Remita, S. Influence of Chemical and Structural Properties of Functionalized Polythiophene-Based Layers on Electrochemical Sensing of Atrazine. *ChemPhysChem* **2012**, *13*, 281−290.
(28) Hui, Y.; Bian, C.; Xia, S.; Tong, J.; Wang, J. Synthesis and Electrochemical Sensing Application of Poly(3,4-Ethylenedioxythiophene)-Based Materials: A Review. *Anal. Chim. Acta* **2018**, *1022*, 1−19.
(29) Strakosas, X.; Wei, B.; Martin, D. C.; Owens, R. M. Biofunctionalization of Polydioxythiophene Derivatives for Biomedical Applications. *J. Mater. Chem. B* **2016**, *4*, 4952−4968.
(30) Verma, K. D.; Sinha, P.; Banerjee, S.; Kar, K. K. *Characteristics of Electrode Materials for Supercapacitors*; Springer Series in Materials Science; Springer, 2020; Vol. *300*, pp 269−285.
(31) Kumar, N.; Ginting, R. T.; Kang, J. W. Flexible, Large-Area, All-Solid-State Supercapacitors Using Spray Deposited PEDOT:PSS/ Reduced-Graphene Oxide. *Electrochim. Acta* **2018**, *270*, 37−47.
(32) Pérez-Mitta, G.; Marmisollé, W. A.; Trautmann, C.; Toimil-Molares, M. E.; Azzaroni, O. An All-Plastic Field-Effect Nanofluidic Diode Gated by a Conducting Polymer Layer. *Adv. Mater.* **2017**, No. 1700972.
(33) Sappia, L. D.; Piccinini, E.; Marmisollé, W.; Santilli, N.; Maza, E.; Moya, S.; Battaglini, F.; Madrid, R. E.; Azzaroni, O. Integration of Biorecognition Elements on PEDOT Platforms through Supramolecular Interactions. *Adv. Mater. Interfaces* **2017**, No. 1700502.
(34) Sappia, L. D.; Piccinini, E.; von Binderling, C.; Knoll, W.; Marmisollé, W.; Azzaroni, O. PEDOT-Polyamine Composite Films for Bioelectrochemical Platforms - Flexible and Easy to Derivatize. *Mater. Sci. Eng., C* **2020**, *109*, No. 110575.
(35) Scotto, J.; Piccinini, E.; von Bilderling, C.; Coria-Oriundo, L. L.; Battaglini, F.; Knoll, W.; Marmisolle, W. A.; Azzaroni, O. Flexible Conducting Platforms Based on PEDOT and Graphite Nanosheets for Electrochemical Biosensing Applications. *Appl. Surf. Sci.* **2020**, *525*, No. 146440.
(36) Zhou, H.; Zhai, H.-J.; Han, G. Superior Performance of Highly Flexible Solid-State Supercapacitor Based on the Ternary Composites of Graphene Oxide Supported Poly(3,4-Ethylenedioxythiophene)-Carbon Nanotubes. *J. Power Sources* **2016**, *323*, 125−133.
(37) Marmisollé, W. A.; Azzaroni, O. Recent Developments in the Layer-by-Layer Assembly of Polyaniline and Carbon Nanomaterials for Energy Storage and Sensing Applications. From Synthetic Aspects to Structural and Functional Characterization. *Nanoscale* **2016**, *8*, 9890−9918.
(38) Tai, C.; Peng, J.-F.; Liu, J.-F.; Jiang, G.-B.; Zou, H. Determination of Hydroxyl Radicals in Advanced Oxidation Processes with Dimethyl Sulfoxide Trapping and Liquid Chromatography. *Anal. Chim. Acta* **2004**, *527*, 73−80.
(39) Chang, Z.; Huang, A.; An, X.; Qian, X. Design and Fabrication of High Performance Supercapacitor with Cellulosic Paper Electrode and Plant-Derived Redox Active Molecules. *Carbohydr. Polym.* **2020**, *244*, No. 116442.
(40) Dong, L.; Xu, C.; Li, Y.; Pan, Z.; Liang, G.; Zhou, E.; Kang, F.; Yang, Q.-H. Breathable and Wearable Energy Storage Based on Highly Flexible Paper Electrodes. *Adv. Mater.* **2016**, *28*, 9313−9319.
(41) Wang, Z.; Lee, Y. H.; Kim, S. W.; Seo, J. Y.; Lee, S. Y.; Nyholm, L. Why Cellulose-Based Electrochemical Energy Storage Devices? *Adv. Mater.* **2020**, No. 2000892.
(42) Nyholm, L.; Nyström, G.; Mihranyan, A.; Strømme, M. Toward Flexible Polymer and Paper-Based Energy Storage Devices. *Adv. Mater.* **2011**, *23*, 3751−3769.

https://doi.org/10.1021/acsaem.1c01517
ACS Appl. Energy Mater. 2021, 4, 9283−9293

(43) Chang, Z.; Yang, Y.; Li, M.; Wang, X.; Wu, Y. Green Energy Storage Chemistries Based on Neutral Aqueous Electrolytes. *J. Mater. Chem. A* **2014**, *2*, 10739−10755.
(44) Verma, K. D.; Banerjee, S.; Kar, K. K. *Characteristics of Electrolytes*; Springer Series in Materials Science; Springer, 2020; Vol. *300*, pp 287−314.
(45) Lyons, M. E. G. *Electroactive Polymer Electrochemistry*, 1st ed.; Lyons, M. E. G., Ed.; Plenum: New York, MA, 1996.
(46) Inzelt, G. *Conducting Polymers: A New Era in Electrochemistry*; Springer-Verlag: Berlin, 2008.
(47) Stavrinidou, E.; Winther-Jensen, O.; Shekibi, B. S.; Armel, V.; Rivnay, J.; Ismailova, E.; Sanaur, S.; Malliaras, G. G.; Winther-Jensen, B. Engineering Hydrophilic Conducting Composites with Enhanced Ion Mobility. *Phys. Chem. Chem. Phys.* **2014**, *16*, 2275−2279.
(48) Schmode, P.; Ohayon, D.; Reichstein, P. M.; Savva, A.; Inal, S.; Thelakkat, M. High-Performance Organic Electrochemical Transistors Based on Conjugated Polyelectrolyte Copolymers. *Chem. Mater.* **2019**, *31*, 5286−5295.
(49) Stavrinidou, E.; Leleux, P.; Rajaona, H.; Khodagholy, D.; Rivnay, J.; Lindau, M.; Sanaur, S.; Malliaras, G. G. Direct Measurement of Ion Mobility in a Conducting Polymer. *Adv. Mater.* **2013**, *25*, 4488−4493.
(50) Talukdar, H.; Bhowal, A. C.; Kundu, S. Percolation Dependent Conducting Behavior of Poly (3,4-Ethylenedioxythiophene): Poly (Styrenesulfonate) in the Presence of Cationic Polyelectrolyte. *Phys. E* **2019**, *107*, 30−37.
(51) Fenoy, G. E.; Bilderling, C.; von Knoll, W.; Azzaroni, O.; Marmisollé, W. A. PEDOT:Tosylate-Polyamine-Based Organic Electrochemical Transistors for High-Performance Bioelectronics. *Adv. Electron. Mater.* **2021**, No. 2100059.
(52) Winther-Jensen, B.; Breiby, D. W.; West, K. Base Inhibited Oxidative Polymerization of 3,4-Ethylenedioxythiophene with Iron-(III)Tosylate. *Synth. Met.* **2005**, *152*, 1−4.
(53) Winther-jensen, B.; West, K. Stability of Highly Conductive Poly-3, 4-Ethylene-Dioxythiophene. *React. Funct. Polym.* **2006**, *66*, 479−483.
(54) Larsen, S. T.; Vreeland, R. F.; Heien, M. L.; Taboryski, R. Characterization of Poly(3,4-Ethylenedioxythiophene):Tosylate Conductive Polymer Microelectrodes for Transmitter Detection. *Analyst* **2012**, *137*, 1831.
(55) Yao, B.; Chandrasekaran, S.; Zhang, J.; Xiao, W.; Qian, F.; Zhu, C.; Duoss, E. B.; Spadaccini, C. M.; Worsley, M. A.; Li, Y. Efficient 3D Printed Pseudocapacitive Electrodes with Ultrahigh MnO 2 Loading. *Joule* **2019**, *3*, 459−470.
(56) Zhao, D.; Zhang, Q.; Chen, W.; Yi, X.; Liu, S.; Wang, Q.; Liu, Y.; Li, J.; Li, X.; Yu, H. Highly Flexible and Conductive Cellulose-Mediated PEDOT:PSS/MWCNT Composite Films for Supercapacitor Electrodes. *ACS Appl. Mater. Interfaces* **2017**, *9*, 13213−13222.
(57) Garcia, D. M. E.; Pereira, A. S. T. M.; Almeida, A. C.; Roma, U. S.; Soler, A. B. A.; Lacharmoise, P. D.; Das Mercês Ferreira, I. M.; Simaõ, C. C. D. Large-Area Paper Batteries with Ag and Zn/Ag Screen-Printed Electrodes. *ACS Omega* **2019**, *4*, 16781−16788.
(58) Jiao, S.; Li, T.; Xiong, C.; Tang, C.; Dang, A.; Li, H.; Zhao, T. A Facile Method of Preparing the Asymmetric Supercapacitor with Two Electrodes Assembled on a Sheet of Filter Paper. *Nanomaterials* **2019**, *9*, No. 1338.
(59) Chen, X.; Jiang, F.; Jiang, Q.; Jia, Y.; Liu, C.; Liu, G.; Xu, J.; Duan, X.; Zhu, C.; Nie, G.; Liu, P. Conductive and Flexible PEDOT-Decorated Paper as High Performance Electrode Fabricated by Vapor Phase Polymerization for Supercapacitor. *Colloids Surf., A* **2020**, *603*, No. 125173.
(60) da Silva, R. J.; Lima, R. M. A. P.; de Oliveira, M. C. A.; Alcaraz-Espinoza, J. J.; de Melo, C. P.; de Oliveira, H. P. Supercapacitors Based on (Carbon Nanostructure)/PEDOT/(Eggshell Membrane) Electrodes. *J. Electroanal. Chem.* **2020**, *856*, No. 113658.

https://doi.org/10.1021/acsaem.1c01517
ACS Appl. Energy Mater. 2021, 4, 9283−9293